Quiet-Sun Magnetism

Probing Deep Photospheric Layers with High Magnetic Sensitivity

Andreas Lagg
and the GREGOR/GRIS team[1]

Max-Planck-Institut für Sonnensystemforschung
Göttingen, Germany

[1] Kiepenheuer Institut für Sonnenphysik (KIS), Freiburg; Leibniz-Institut für Astrophysik Potsdam (AIP); Germany
Instituto de Astrofísica de Canarias (IAC), Tenerife, Spain

Hinode-10 Meeting

Nagoya

Sep-05 2016

Relevance

- QS magnetism covers >90% of solar surface (even during maxima); 15% in inter-network
- crucial to understand the solar global magnetism
- e.g. origin: local (surface) dynamo or cascade from global dynamo?

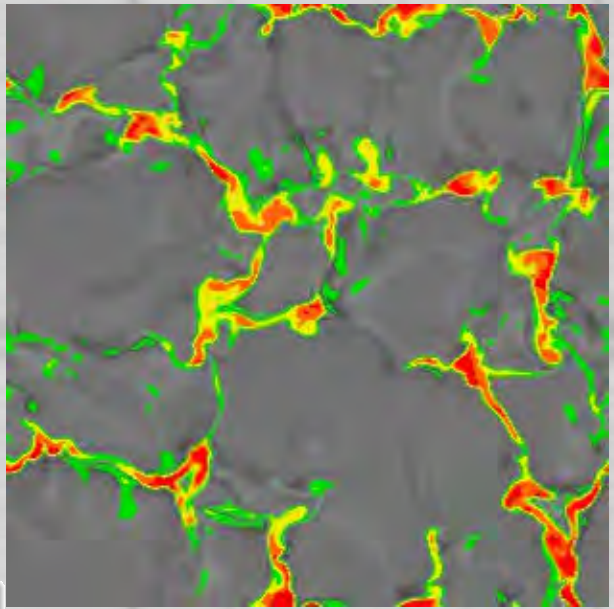

M. Rempel (MURaM)

Summary angular distributions (Tab. 2 from Steiner & Rezaei, 2012)

no.	authors	instrument/ simulation	line [nm]	angular distribution	$\langle B^{\mathrm{T}}_{\mathrm{app}} \rangle$/ $\langle \lvert B^{\mathrm{L}}_{\mathrm{app}} \rvert \rangle$
1	Lites et al. (2007, 2008)	SOT/SP	630	predominantly horizontal	5
2	Orozco Suárez et al. (2007)	SOT/SP	630	predominantly horizontal	2.1
3	Martínez González et al. (2008)	VTT/TIP	1560	isotropic distribution	—
4	Beck & Rezaei (2009)	VTT/TIP	1560	predominantly vertical	0.42
5	Asensio Ramos (2009)	SOT/SP	630	isotropic for weak fields	—
6	Danilovic et al. (2010)	SOT/SP	630	predominantly horizontal	5.8
7	Stenflo (2010)	SOT/SP	630	predominantly vertical	—
8	Ishikawa & Tsuneta (2011)	SOT/SP	630	predominantly vertical	0.86
9	Borrero & Kobel (2011)	SOT/SP	630	undeterminable	—
10	Borrero & Kobel (2012)	SOT/SP	630	non-isotropic	—
11	Steiner et al. (2008)	h20	630	predominantly hor-	4.3 (2.8)
		v10	630	izontal	1.6 (1.5)
12	Danilovic et al. (2010)	C mf=3	630	predominantly hor-	9.8 (3.5)
		C+B_{ver}	630	izontal	4.2 (2.6)

Summary of observations

Summary of observations

Reason 1: Sensitivity of polarimeters

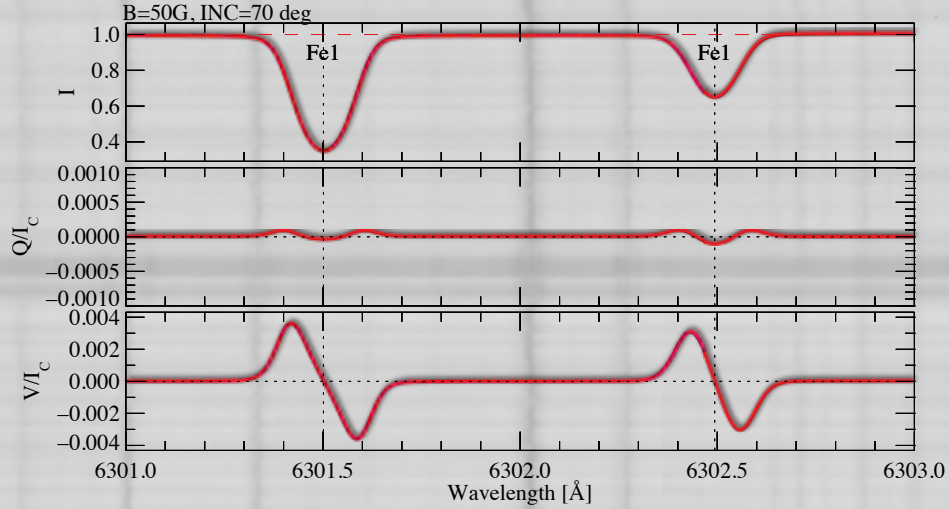

Reason 1: Sensitivity of polarimeters

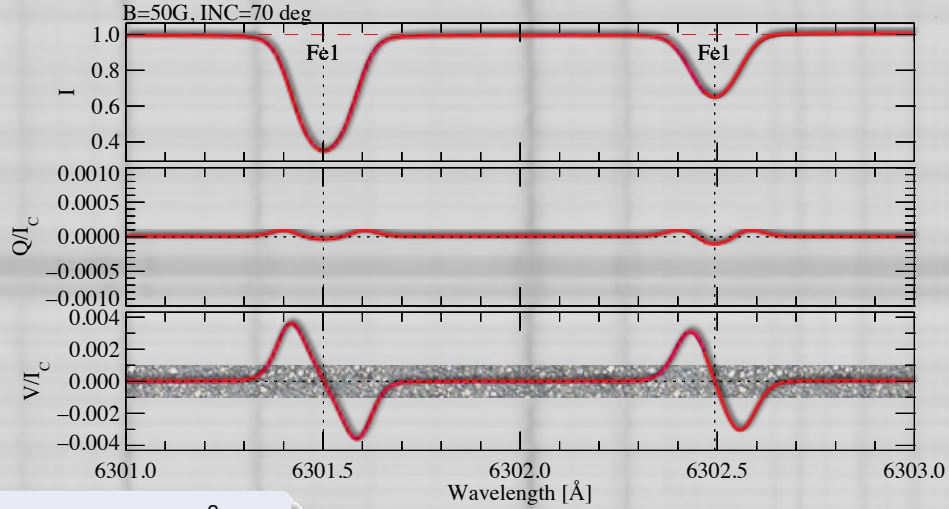

add noise: $10^{-3} I_C$

Reason 1: Sensitivity of polarimeters

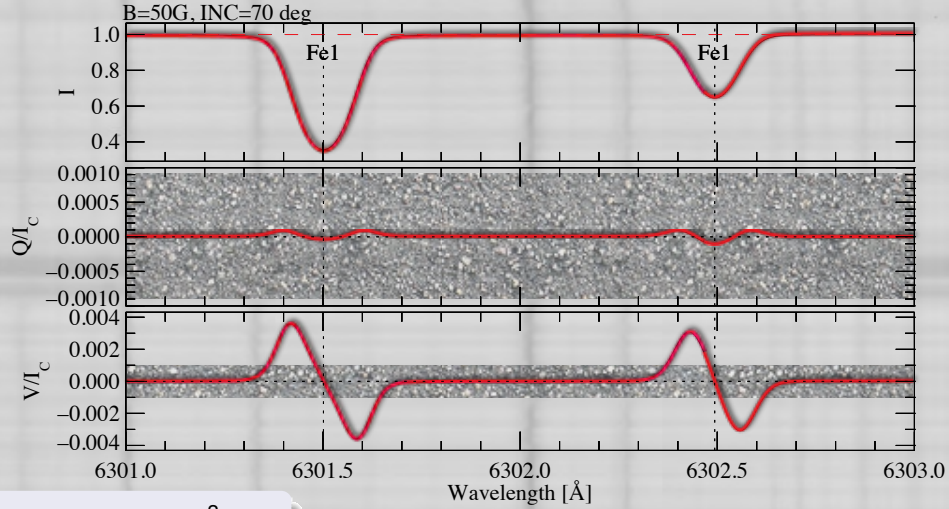

add noise: $10^{-3} I_C$

Reason 2: Bias introduced by Zeeman effect

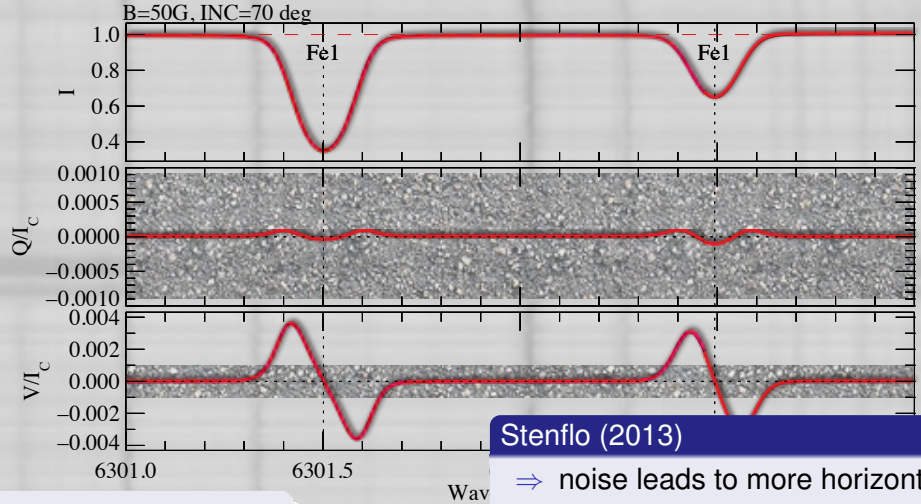

add noise: $10^{-3} I_C$

Stenflo (2013)

- $\Rightarrow$ noise leads to more horizontal fields
- $\Rightarrow$ apparent flux: $25\times$ higher in B_h

Reasons 3+4: Cancellation & Methods

Signal cancellation

insufficient spatial resolution for Zeeman diagnostics

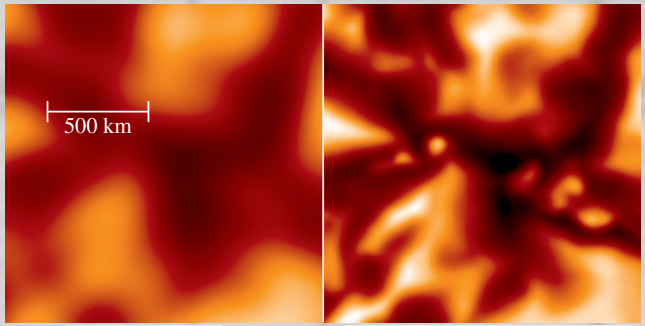

Hinode GREGOR / Solar-C

Analysis methods

- Zeeman vs. Hanle
- selection of profiles (σ-level)
- inversions
  - ME vs. height dependent
  - filling factor
- direct techniques (e.g. line ratio)

Reasons 3+4: Cancellation & Methods

Signal cancellation

insufficient spatial resolution for Zeeman diagnostics

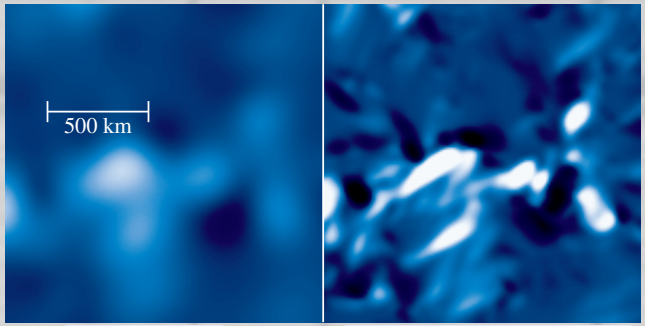

Hinode

GREGOR / Solar-C

Analysis methods

- Zeeman vs. Hanle
- selection of profiles (σ-level)
- inversions
  - ME vs. height dependent
  - filling factor
- direct techniques (e.g. line ratio)

Reason 5: Height dependent B_v & B_h

B_v vs. B_h

depends strongly on

- spectral line selection
- analysis method (height dependent inversion vs. ME)
- heliocentric angle (higher opacity at limb)

small scale dynamo

- MHD: $P(\gamma) \propto \sin\gamma$ (e.g. Vögler & Schüssler, 2007)
- height dependent (Rempel, 2014)

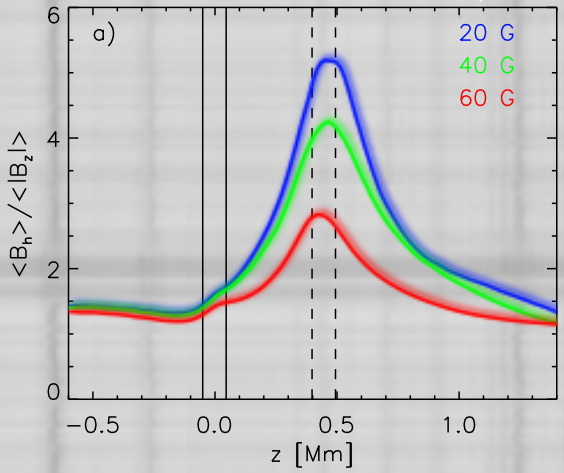

Rempel (2014)

Possible solutions?

Increase spatial resolution

- larger telescope aperture

Increase signal/noise ratio

- more photons
- better polarimeter
- more sensitive spectral lines

Remove height bias

- select lines with narrow and known formation height
- increase height resolution

Remove model ambiguities

- select simple, bias-free analysis method without

Recent results from GREGOR / GRIS

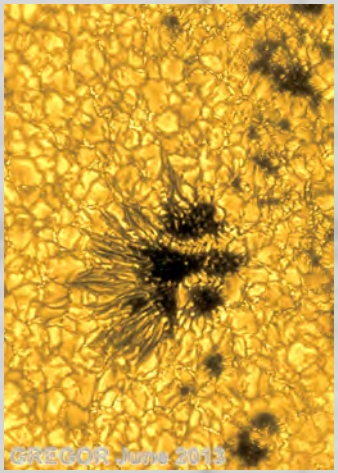

GREGOR Infrared Spectrograph (GRIS; Collados et al., 2012)

GRIS fact sheet

- WL-range 1–2.3μm
- sensitivity $< 10^{-4}$
- $\lambda/\Delta\lambda \approx 120\,000$ (@1.56 μm)
- mounted at 1.5 m GREGOR telescope
- $0\farcs18$–$0\farcs30$ resolution

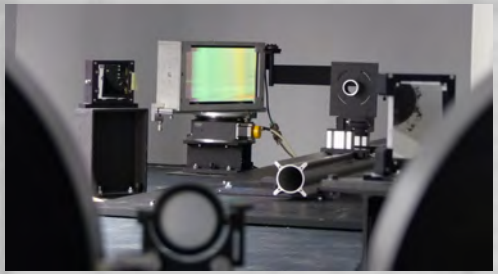

Scan of quiet sun region (2015-Sep-17)

- FFT rebinned: 0.″135 pixelsize

→ 0.″20 pixelsize (seeing limited: 0.″40)

- noise level reduction: $4 \cdot 10^{-4}$ I_C

→ $2.7 \cdot 10^{-4}$ I_C

→ no loss in spatial resolution

- spectral binning

→ $\times 2$ (oversampling)

→ $2.1 \cdot 10^{-4}$ I_C

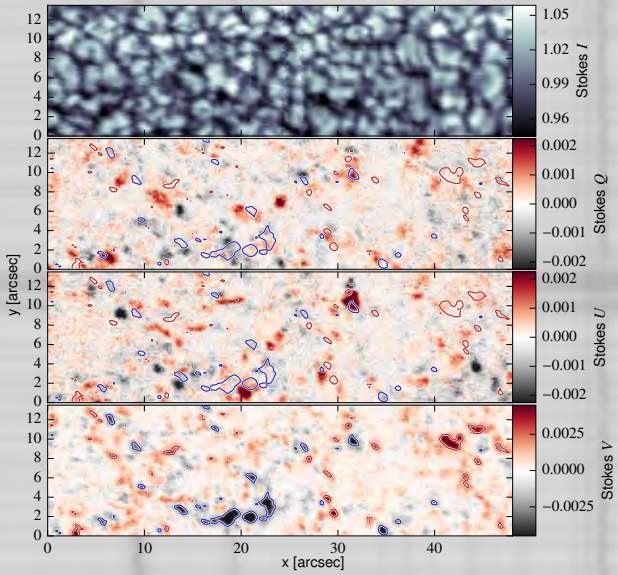

Comparison: GRIS vs. SOT/SP: Stokes Maps

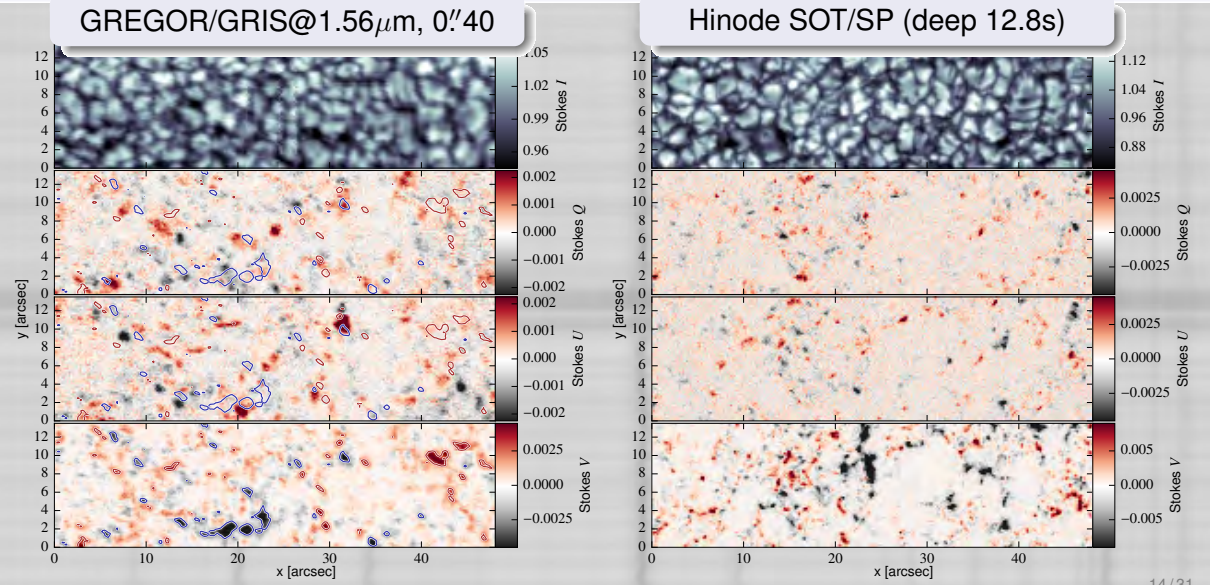

Comparison: GRIS vs. SOT/SP: LP/CP Coverage

$V \geq 3\sigma$ $Q, U \geq 3\sigma$ $Q, U, V \geq 3\sigma$

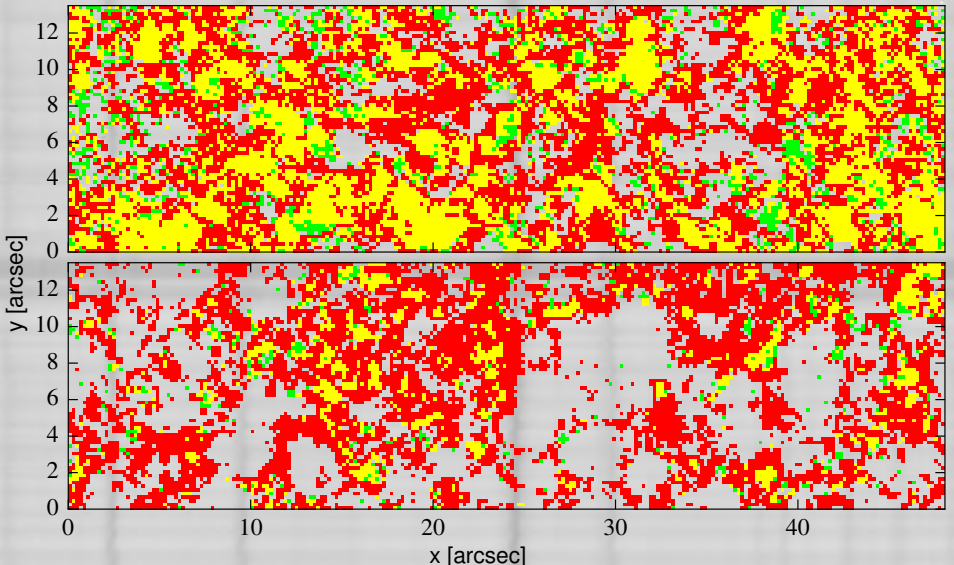

GREGOR/GRIS
4.8 s, 0.″40, $2 \cdot 10^{-4}$

Hinode SOT/SP
12.8 s, 0.″40, $7 \cdot 10^{-4}$

Stokes signal levels

Comparison GRIS ↔ Hinode SOT/SP

σ-level	GRIS [%]		LP and CP	LP or CP	SOT/SP [%]		LP and CP	LP or CP
	LP	CP			LP	CP		
3σ	39.7	73.0	33.1	79.7	9.8	49.3	7.7	51.4
4σ	18.4	57.0	13.9	61.5	4.2	37.1	3.1	38.2
5σ	9.2	44.2	6.2	47.2	2.1	28.5	1.5	29.1

Simple diagnostic techniques: MLR - field strength

Magnetic Line Ratio (Solanki et al., 1992)

$$\mathrm{MLR} = \frac{g_{\mathrm{eff}}(15652)\, V_{\mathrm{max}}(15648)}{g(15648)\, V_{\mathrm{max}}(15652)}$$

Requirements:

- spectral lines identical except for Landé factor
- 2 distinct components:
  (1) magnetized, (2) field-free
- small gradients in $\log \tau$

$\rightarrow$ not fulfilled for Fe I 1.56 line pair

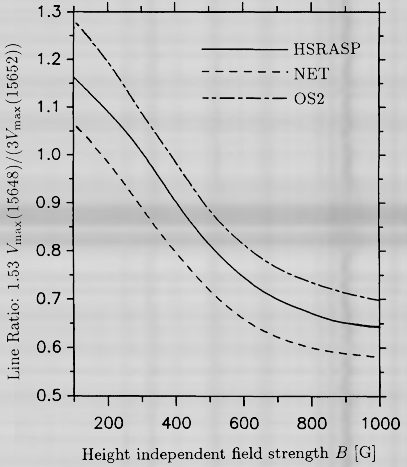

Simple diagnostic techniques: MLR - field strength

Magnetic Line Ratio (Solanki et al., 1992)

$$\mathrm{MLR} = \frac{g_{\mathrm{eff}}(15652)\, V_{\mathrm{max}}(15648)}{g(15648)\, V_{\mathrm{max}}(15652)}$$

Requirements:

- spectral lines identical except for Landé factor
- 2 distinct components:
  (1) magnetized, (2) field-free
- small gradients in $\log \tau$

$\rightarrow$ not fulfilled for Fe I 1.56 line pair

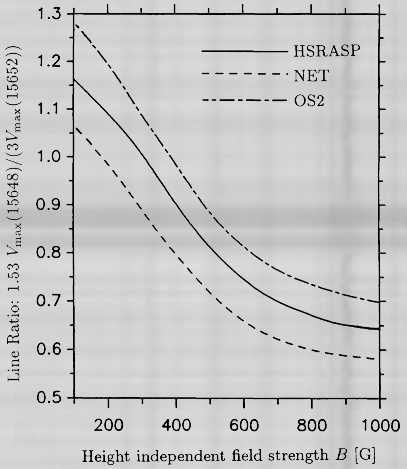

Simple diagnostic techniques: MLR - field strength

Magnetic Line Ratio (Solanki et al., 1992)

$$\mathrm{MLR} = \frac{g_{\mathrm{eff}}(15652)\, V_{\mathrm{max}}(15648)}{g(15648)\, V_{\mathrm{max}}(15652)}$$

Requirements:

- spectral lines identical except for Landé factor
- 2 distinct components:
  (1) magnetized, (2) field-free
- small gradients in $\log \tau$

→ not fulfilled for Fe I 1.56 line pair

→ BUT: similar formation height, narrow formation height range, similar thermal properties

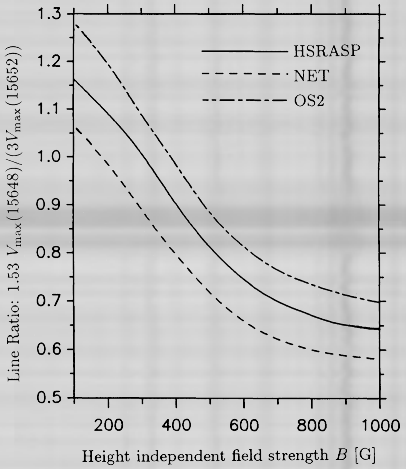

MLR analysis - select “normal” profiles

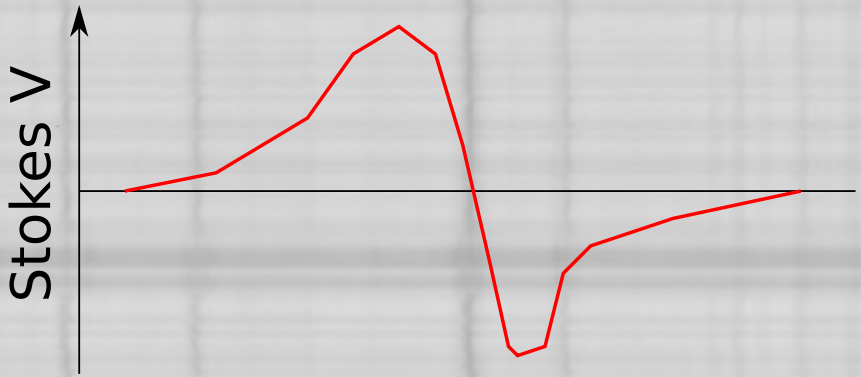

MLR analysis - select “normal” profiles

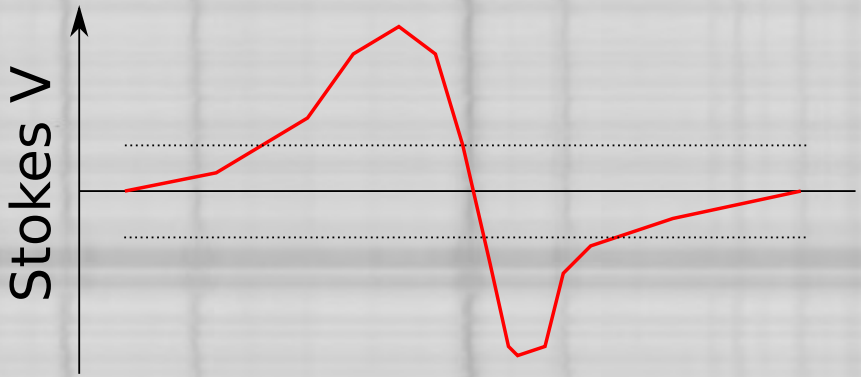

noise threshold 3σ

MLR analysis - select “normal” profiles

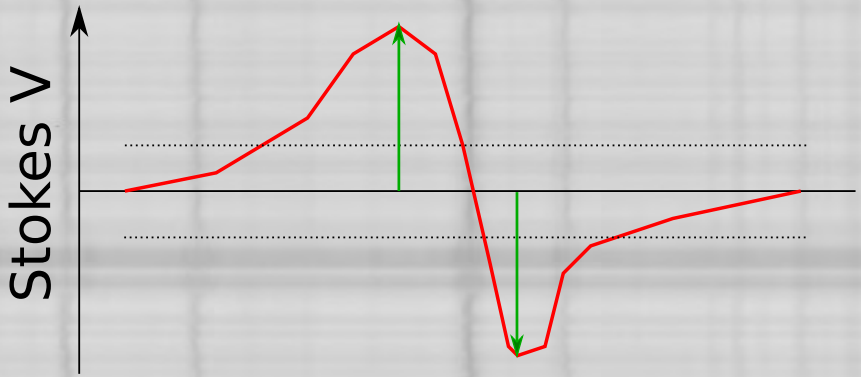

noise threshold 3σ

small amplitude asym. δa

MLR analysis - select “normal” profiles

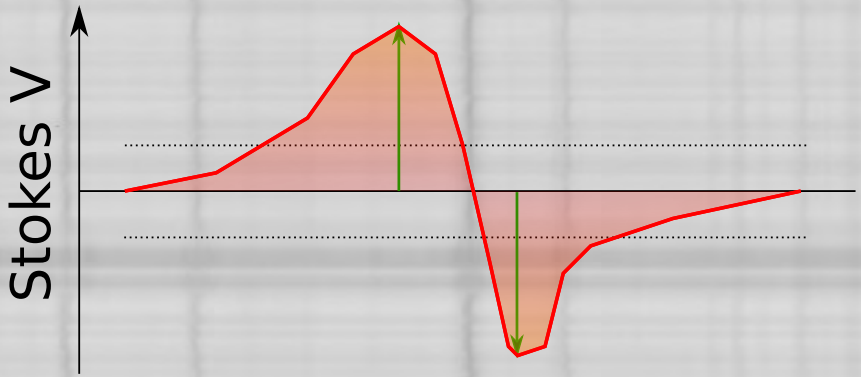

noise threshold 3σ

small amplitude asym. δa

small area asym. δA

MLR analysis - select “normal” profiles

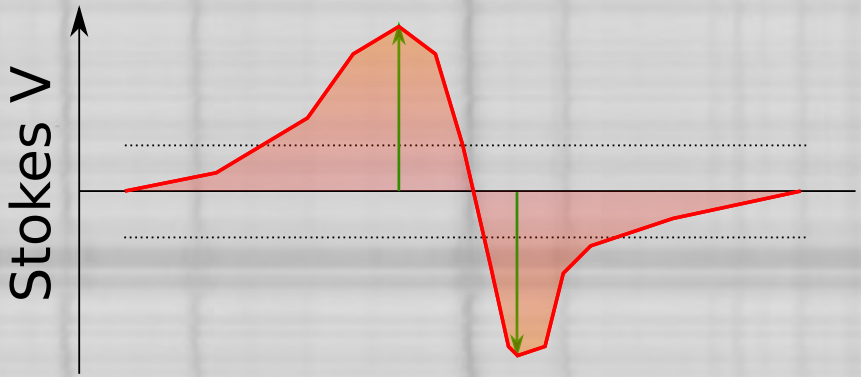

noise threshold 3σ

small amplitude asym. δa

small area asym. δA

(43.7% of the profiles)

Stokes Profiles: Red: MLR≈0.6, large V_{max}, Yellow ×3: MLR≈0.6, small V_{max}

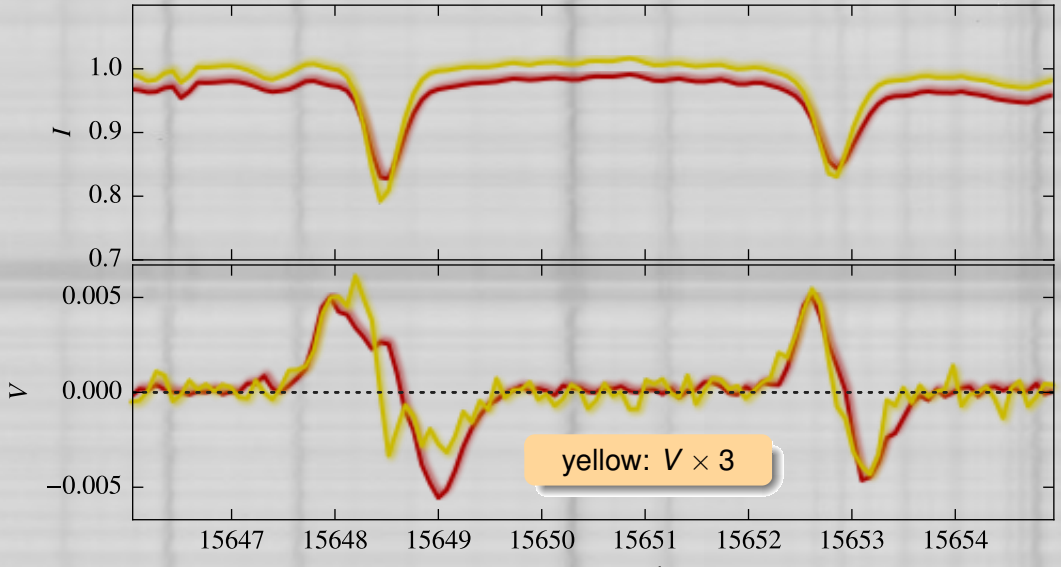

Stokes Profiles: Red: MLR≈0.6, large V_{max}, Yellow ×3: MLR≈0.6, small V_{max}

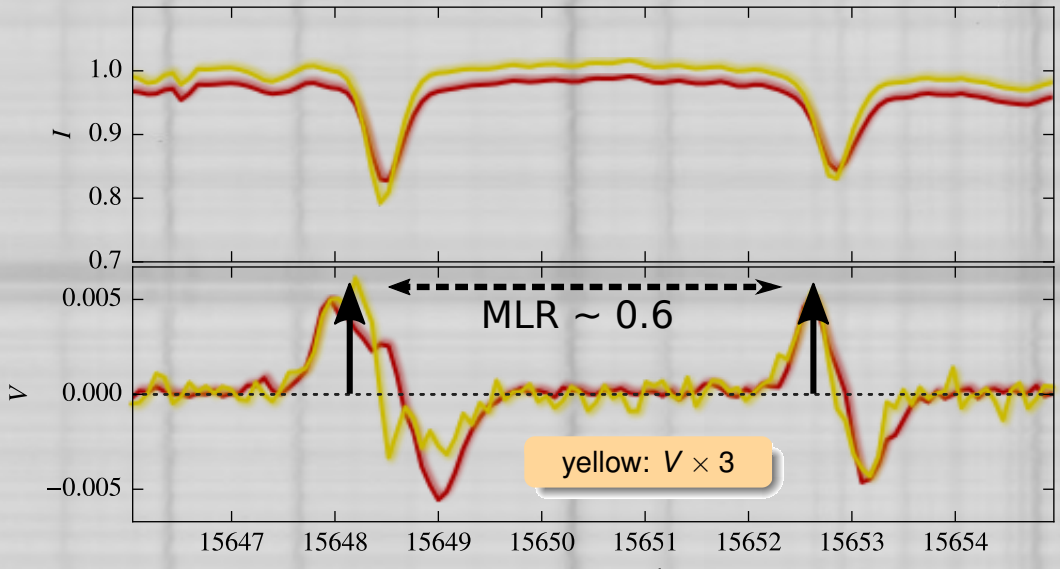

MLR Fe I 15648 / Fe I 15652

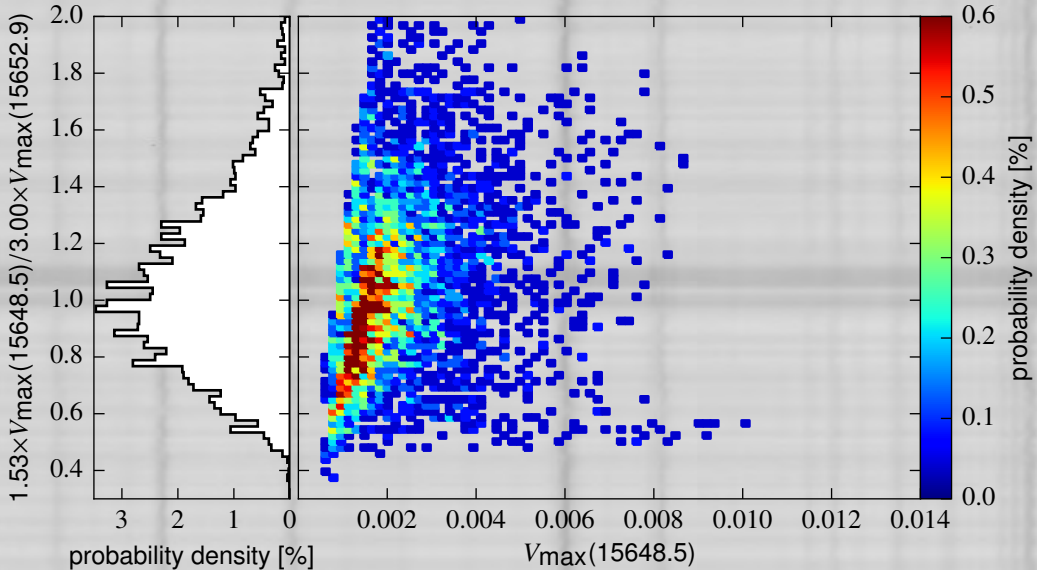

Different MLR regions

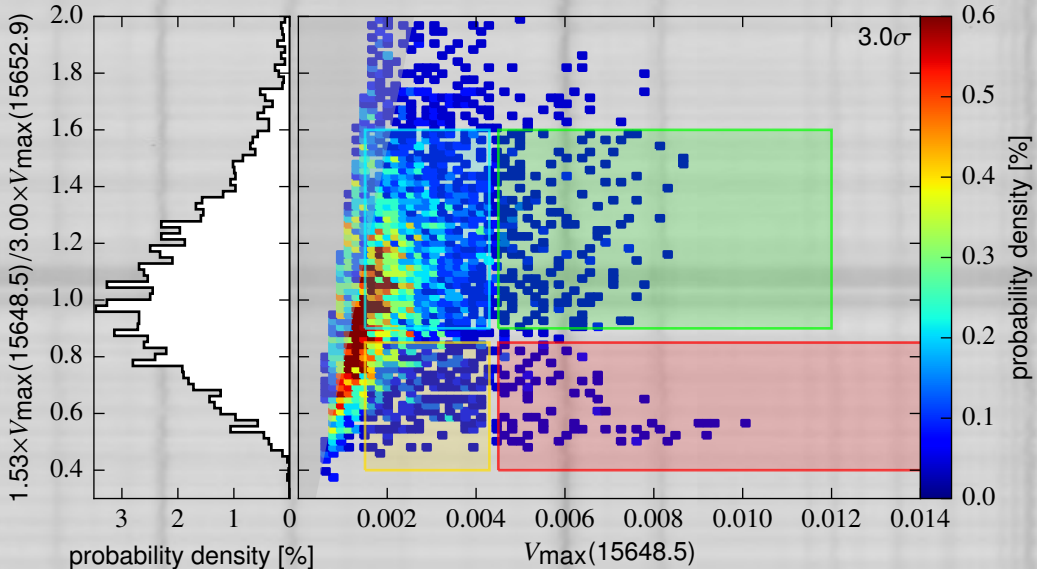

Different MLR regions

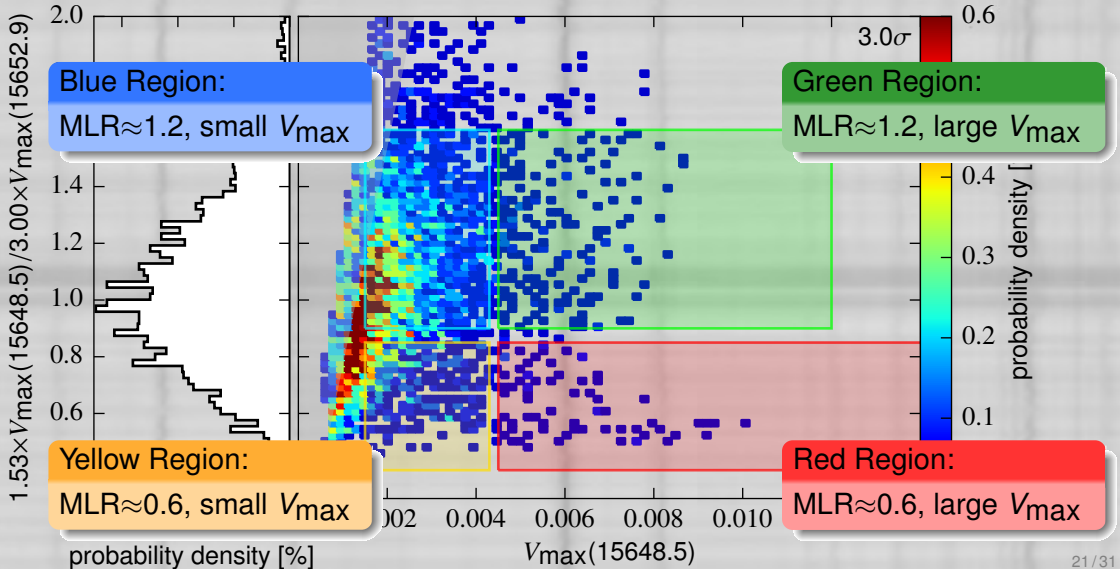

Different MLR regions

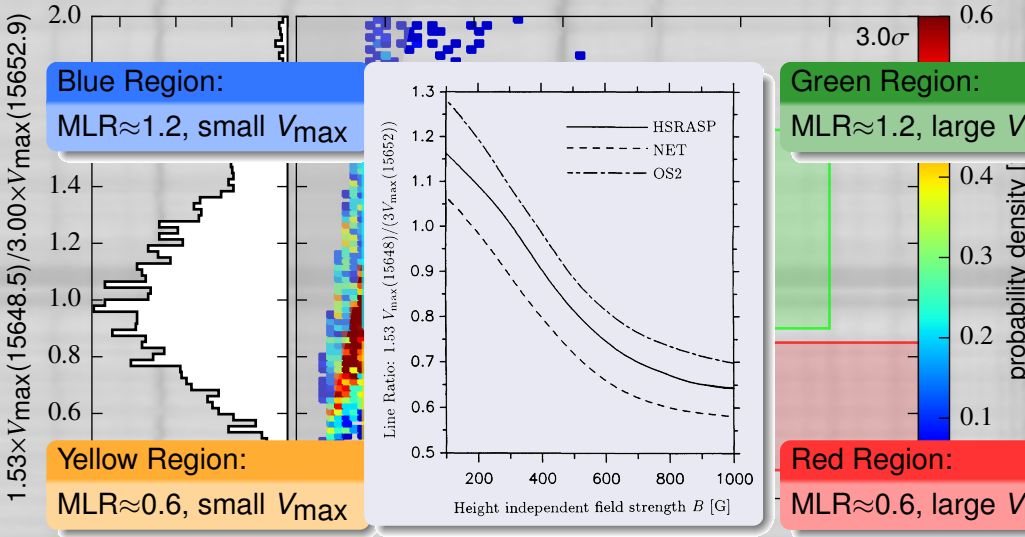

Different MLR regions

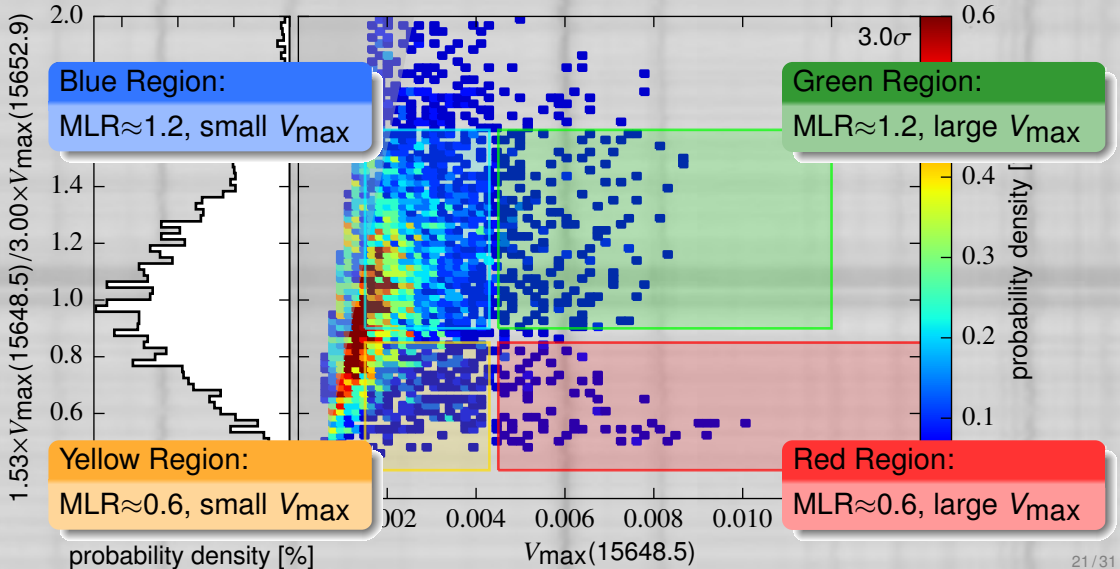

Different MLR regions - Where?

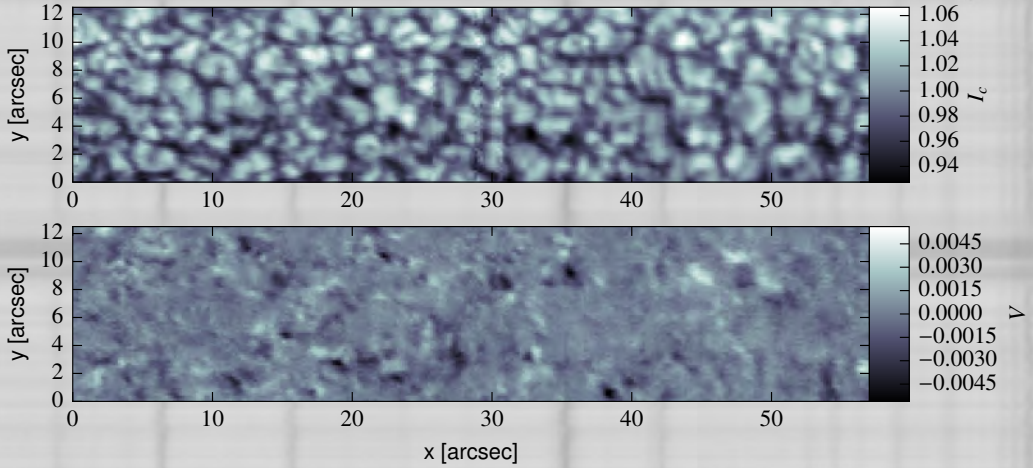

MLR≈1.2, small V_{max} (hG) | MLR≈1.2, large V_{max} (hG) | MLR≈0.6, small V_{max} (kG) | MLR≈0.6, large V_{max} (kG)

Different MLR regions - Where?

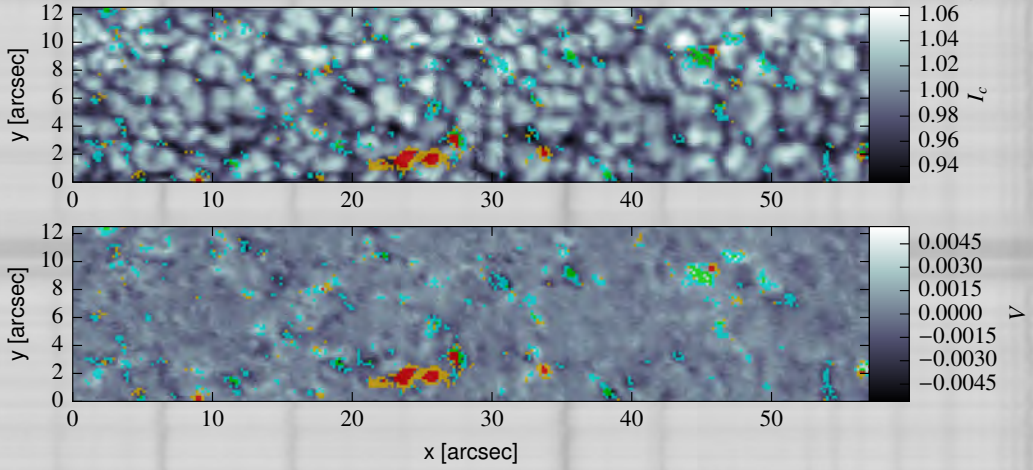

MLR≈1.2, small V_{max} (hG) | MLR≈1.2, large V_{max} (hG) | MLR≈0.6, small V_{max} (kG) | MLR≈0.6, large V_{max} (kG)

Different MLR regions - Where?

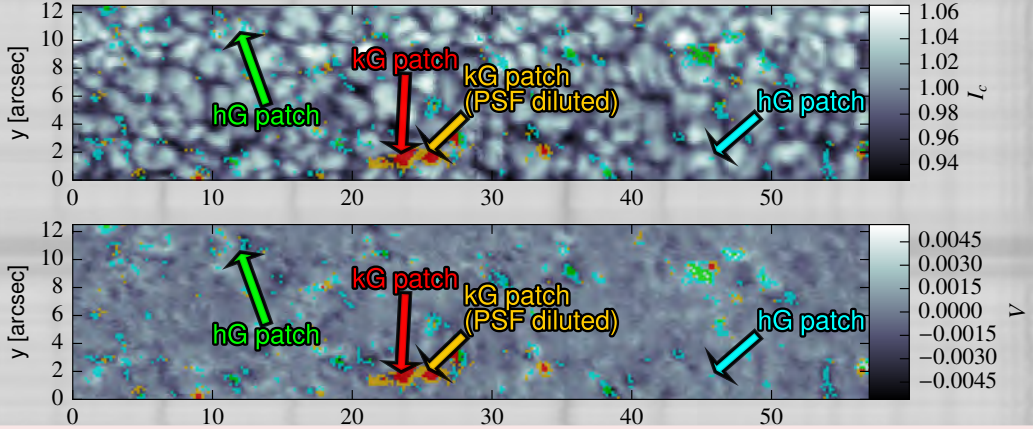

some kG patches (red); surrounded by yellow halo; ubiquitous weak fields (green & blue)

MLR≈1.2, small V_{max} (hG) | MLR≈1.2, large V_{max} (hG) | MLR≈0.6, small V_{max} (kG) | MLR≈0.6, large V_{max} (kG)

Test using MHD Quiet Sun simulations (SSD+IMaX run)

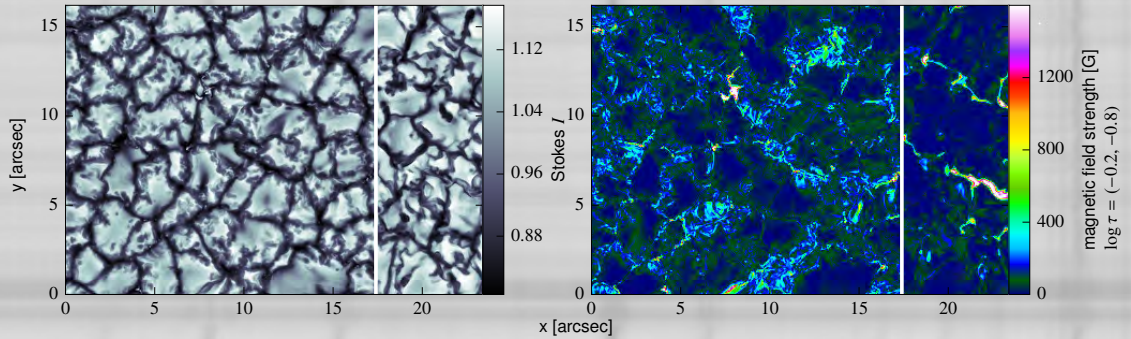

MHD simulations: SSD+IMaX run

- Rempel (2014): O16bM
- Riethmüller et al. (2016)

Test using MHD Quiet Sun simulations (SSD+IMaX run)

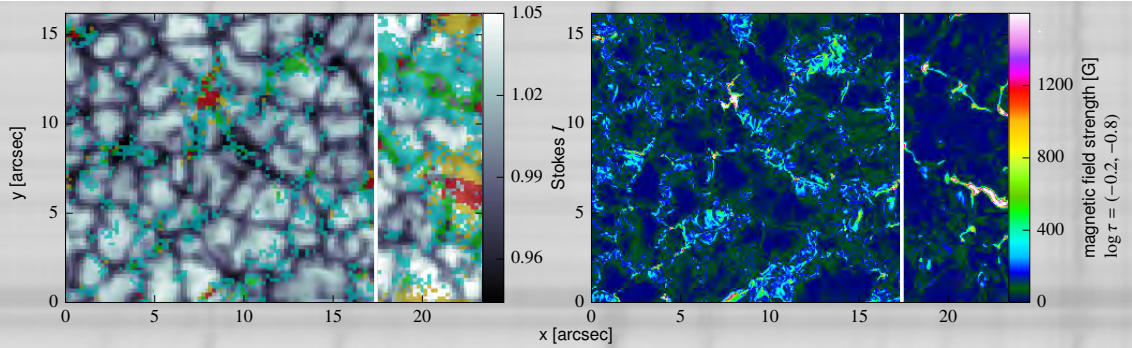

spatial degrading

- GREGOR-PSF + 0.25″ Gaussian + Lorentzian wings

→ match contrast, resolution, I_c histogram

spectral degrading

- 12% straylight
- 150 mÅ Gauss

MLR≈1.2, small V_{max} (hG) MLR≈1.2, large V_{max} (hG) MLR≈0.6, small V_{max} (kG) MLR≈0.6, large V_{max} (kG)

MLR (SSD + IMaX run, degraded)

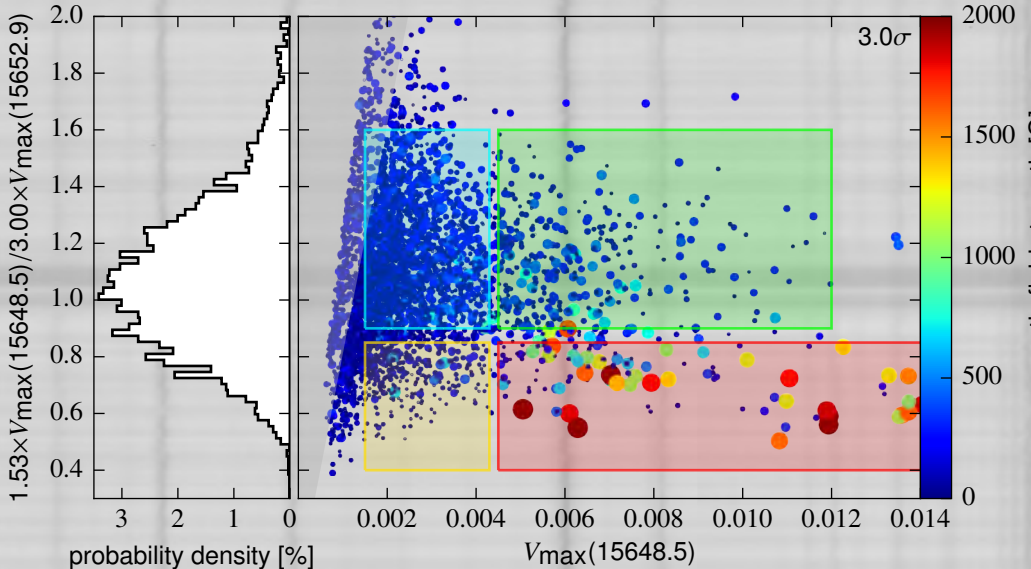

MLR (SSD + IMaX run, degraded)

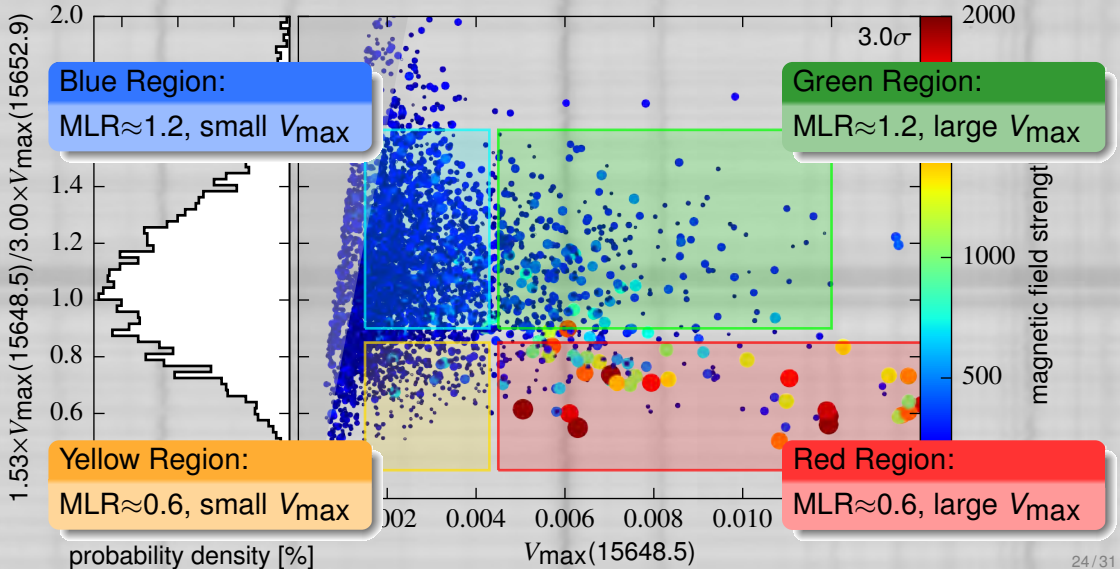

B strength (SSD + IMaX run)

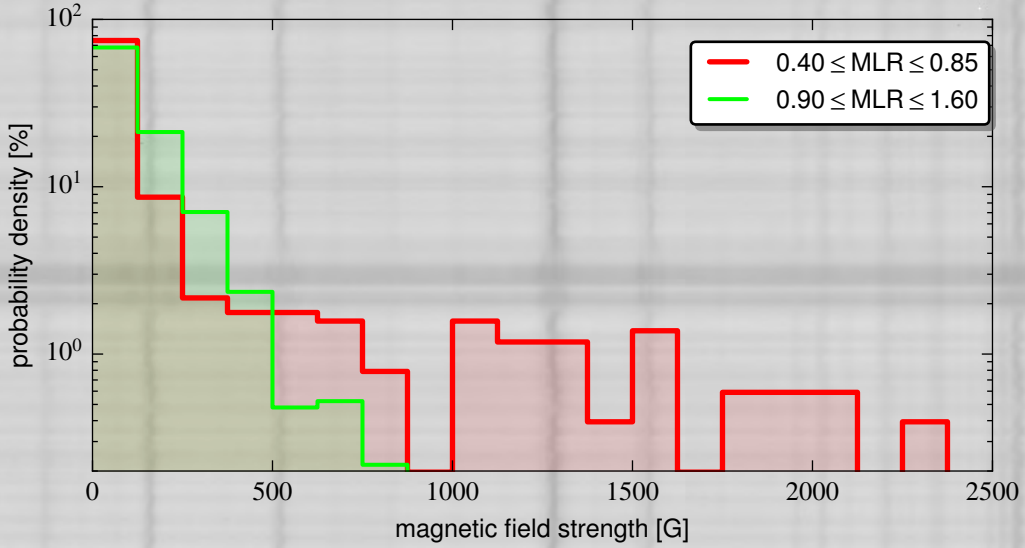

Simple diagnostic techniques: LP/CP - inclination

LP/CP ratio (Solanki et al., 1992)

$$\mathrm{LP/CP} = \frac{\sqrt{Q_{\max}^2 + U_{\max}^2}}{V_{\max}}$$

1. depends only on γ if
   - B sufficiently strong (≥ 1 kG)
   - small gradients
2. depends on γ and B for weaker fields

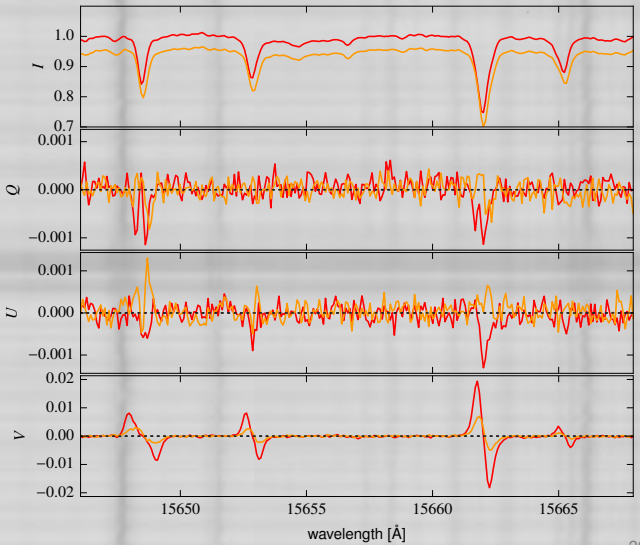

GRIS: LP/CP for Fe I 15648

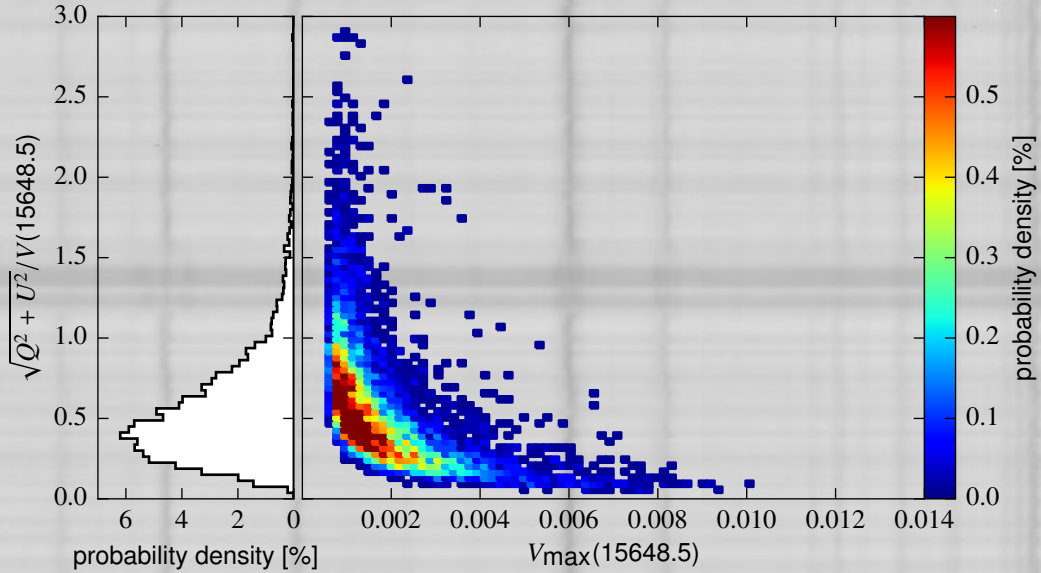

MHD (SSD+IMaX, degraded): LP/CP for Fe I 15648

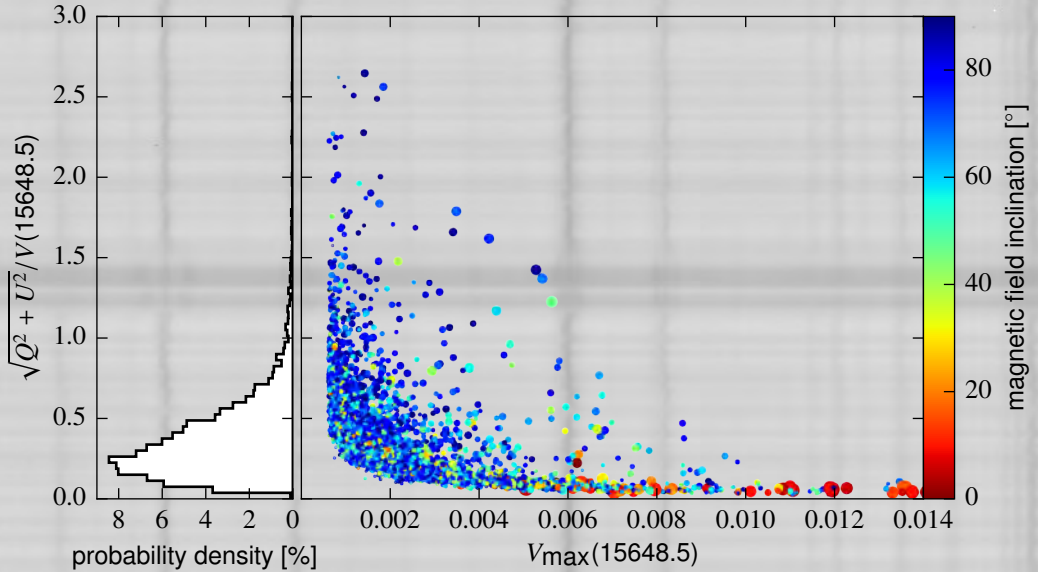

B inclination (SSD + IMaX run)

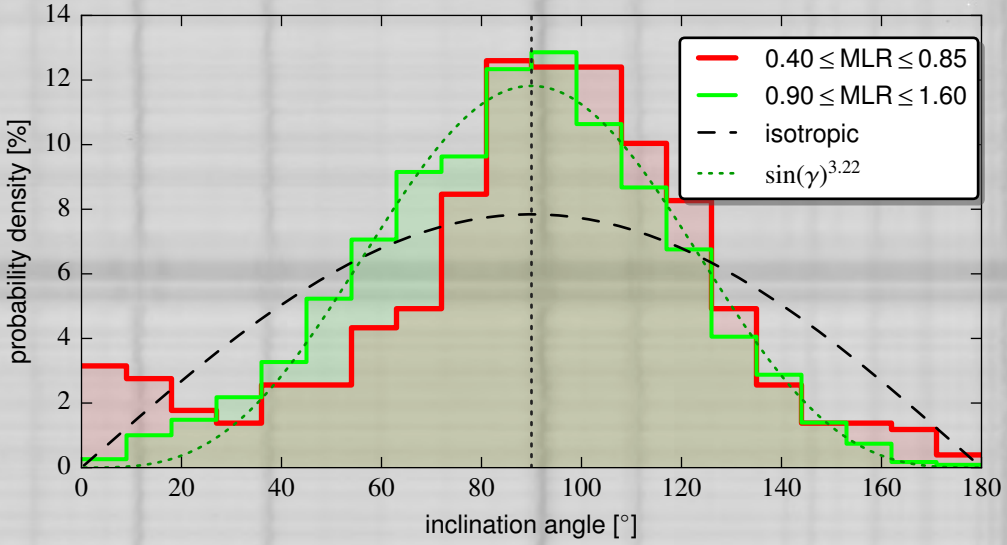

Summary: Quiet Sun Stokes Profiles

Noise Statistics: GRIS↔Hinode

- noise level $2.1 \cdot 10^{-4}$ (0.″40)
- TP: $\approx$ 80% above 3σ (cf. Hinode 12.8 s scan: 51%)
- CP: $\approx$ 73% above 3σ (cf. Hinode 12.8 s scan: 49%)
- LP: $\approx$ 40% above 3σ (cf. Hinode 12.8 s scan: 10%)

$\rightarrow$ more reliable inversions are now possible

MLR & LP/CP ratio

- some kG patches resolved (vertical fields)
- ”PSF-ring” around kG patches
- hG patches ubiquitous
- good agreement with SSD runs $\rightarrow$ some kG patches missing

Proper PSF deconvolution critical for correct interpretation of results!

Future instrumental improvements

- GREGOR/GRIS: reach diffraction limit
- Sunrise III: increase height resolution

Bibliography

Asensio Ramos, A. 2009, ApJ, 701, 1032

Asensio Ramos, A. & Martínez González, M. J. 2014, A&A, 572, A98

Asensio Ramos, A. & Trujillo Bueno, J. 2005, ApJL, 635, L109

Asensio Ramos, A., Trujillo Bueno, J., & Landi Degl'Innocenti, E. 2008, ApJ, 683, 542

Berdyugina, S. V. & Fluri, D. M. 2004, A&A, 417, 775

Bommier, V., et al. 2005, A&A, 432, 295

Borrero, J. M. & Kobel, P. 2013, A&A, 550, A98

Buehler, D., Lagg, A., & Solanki, S. K. 2013, A&A, 555, A33

Collados, M., et al. 2012, Astronomische Nachrichten, 333, 872

Danilovic, S., van Noort, M., & Rempel, M. 2016, A&A, submitted

Faurobert, M., et al. 2001, A&A, 378, 627

Faurobert-Scholl, M., et al. 1995, A&A, 298, 289

Ishikawa, R. & Tsuneta, S. 2011, ApJ, 735, 74

Kleint, L., et al. 2010, A&A, 524, A37

Lagg, A., et al. 2009, in ASP Conf. Ser., Vol. 415, The Second Hinode Science Meeting: Beyond Discovery-Toward Understanding, ed. Lites, B., et al., 327

Lites, B. W., et al. 2008, ApJ, 672, 1237

Martínez González, M. J., et al. 2008, A&A, 479, 229

Martínez González, M. J., et al. 2016, A&A GREGOR issue, accepted

Orozco Suárez, D. & Bellot Rubio, L. R. 2012, ApJ, 751, 2

Orozco Suárez, D., et al. 2007, Publications of the Astronomical Society of Japan, 59, 837

Orozco Suárez, D. & Katsukawa, Y. 2012, ApJ, 746, 182

Rempel, M. 2014, ApJ, 789, 132

Riethmüller, T., et al. 2016, ApJ, in preparation

Schmidt, W., et al. 2012, Astronomische Nachrichten, 333, 796

Shapiro, A. I., et al. 2011, A&A, 529, A139

Shchukina, N. & Trujillo Bueno, J. 2003, in ASP Conf. Ser., Vol. 307, Solar Polarization, ed. Trujillo-Bueno, J. & Sanchez Almeida, J., 336

Solanki, S. K., Rüedi, I. K., & Livingston, W. 1992, A&A, 263, 312

Steiner, O. & Rezaei, R. 2012, in ASP Conf. Ser., Vol. 456, Fifth Hinode Science Meeting, ed. Golub, L., De Moortel, I., & Shimizu, T., 3

Stenflo, J. O. 2010, A&A, 517, A37

Stenflo, J. O. 2013, The Astronomy and Astrophysics Review, 21, 66

Stenflo, J. O. 2014, in ASP Conf. Ser., Vol. 489, Solar Polarization 7, ed. Nagendra, K. N., et al., 3

Trujillo Bueno, J., Shchukina, N., & Asensio Ramos, A. 2004, Nature, 430, 326

Vögler, A. & Schüssler, M. 2007, A&A, 465, L43